Supplementary Information for:

Physically Covariant, Curvilinear Thick-mask Model for Full-chip Computational Lithography

Haofeng Chen[1], Shaopeng Guo[1], Kaixuan Su[1], Song Zhang[1,2], Hao Jiang[1, *], David H. Wei[2,3, *], and Shiyuan Liu[1,2, *]

[1] School of Mechanical Science and Engineering, Huazhong University of Science and Technology, Wuhan 430074, China.

[2] Yuwei Optica Co., Ltd., Wuhan, 430070, Hubei, China.

[3] Quantica Computing LLC, San Jose, California 95131, USA

*hjiang@hust.edu.cn

*david.hq.wei@gmail.com

*shyliu@hust.edu.cn

S1. Analysis of near-field accuracy for the Manhattanisation thick-mask model

Fig. S1 quantitatively illustrates the dependence of near-field errors in the Manhattanisation thick-mask model on the Maximum Edge Displacement (MED), using rigorous FDTD simulations of the curvilinear mask in Fig 6c as the benchmark. When the MED is reduced from 20 nm to 4 nm, the RMS error of the near-field amplitude converges from 0.09911 to 0.06. Similarly, decreasing the MED from 20 nm to 6 nm lowers the MA error from 0.9652 to 0.3445. These results demonstrate that geometric distortion induced by Manhattanisation constitutes one of the primary sources of thick-mask modelling error. Consequently, strict control of MED is imperative to ensure model fidelity when applying Manhattanisation-based preprocessing to curvilinear thick-mask simulations.

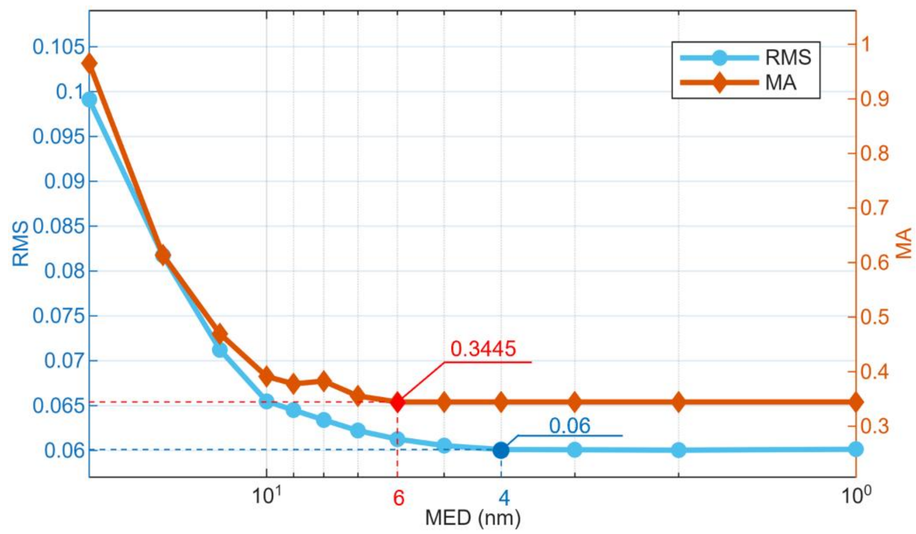

Fig. S1 Convergence curves of the RMS and MA as functions of the MED.

S2. Validation of model applicability

Fig. S2 compares the near-field distributions generated by the proposed and FDTD models for various curvilinear layouts and critical dimensions (CDs), illustrated using the $\mathbf{E_X^X}$ component. Notably, the single-exposure CD limit is 38 nm, constrained by the NA of the projection lens in the computational lithography imaging system. Simulations demonstrate comparable deviations between the proposed model and benchmark across varying CD values and layouts, validating the model's universality.

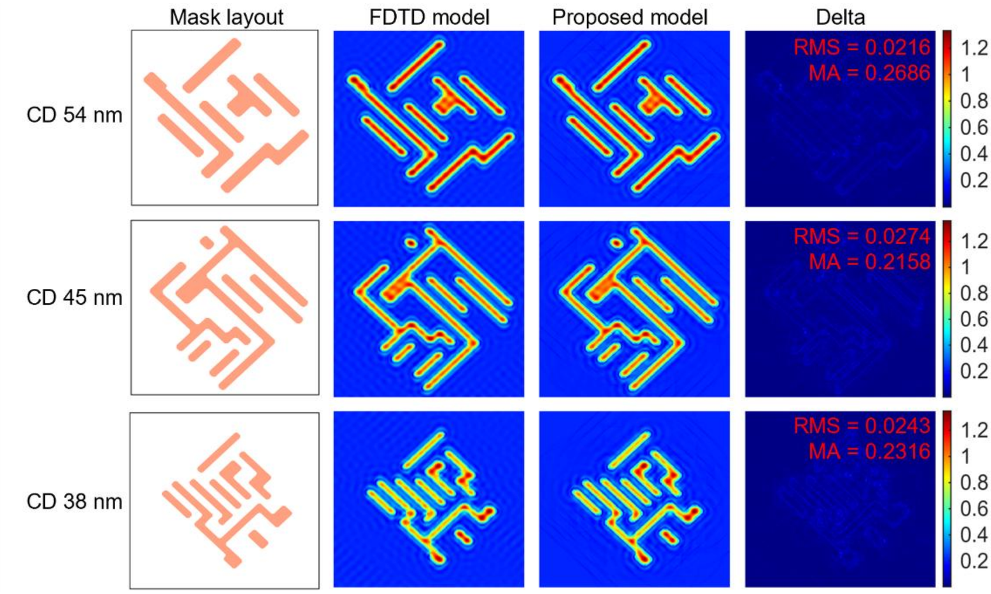

Fig. S2 Deviation analysis of the proposed model versus FDTD near-field for various CDs and mask patterns (using the $\mathbf{E}_\mathbf{X}^\mathbf{X}$ field as an example).

S3. Validation of physical covariance

Fig. S3 displays near-fields generated by the proposed model for the test mask in Fig. 8b after coordinate translation or rotation, along with the corresponding distributions after they are restored to the initial coordinates via inverse transformation.

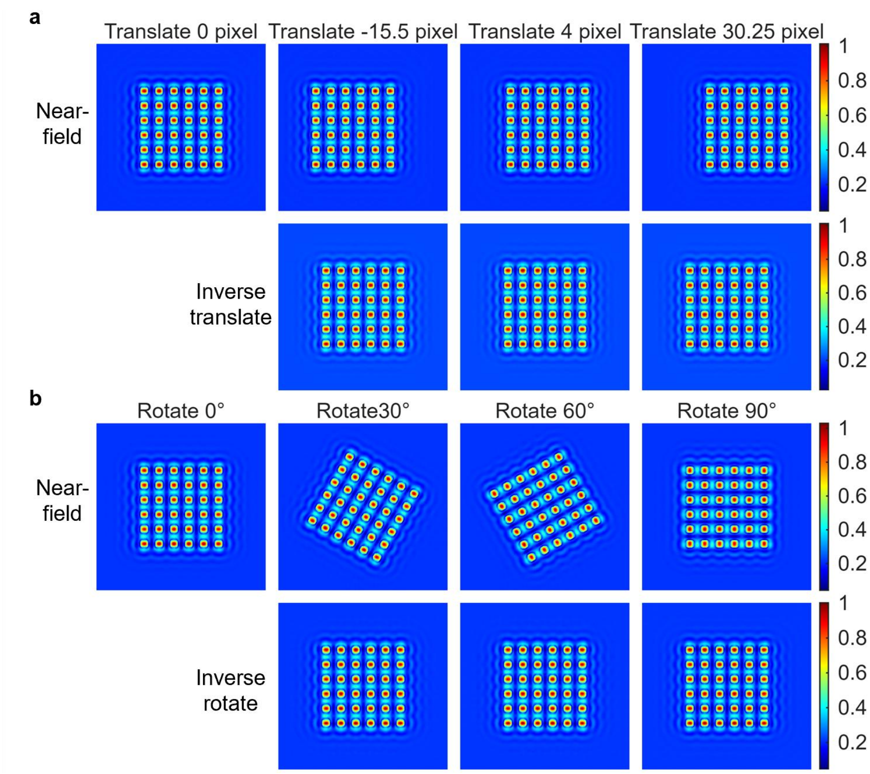

Fig. S3 Near-field evolution under test mask coordinate transformations. **a** Near-fields resulting from the test mask after being translated in the x-direction by 0 pixels, -15.5 pixels, 4 pixels, 30.25 pixels, respectively. **b** Near-field evolution under mask rotations at 0°, 30°, 60° and 90°.

S4. Evaluation of the rigorous simulation domain

Fig. S4 shows the variation curves of RMS and MA errors for the reference mask near-field with increasing simulation domain size. Each error computed relative to the result obtained from the previous (smaller) domain size as the benchmark. At a wavelength of 193 nm, the RMS error of the electromagnetic field converges to 1.82×10^{-4} as the simulation domain expands from 2 to 16 wavelengths. The MA error quickly decreases to 0.0174 by 18 wavelengths, then slowly converges to 0.0082 at 38 wavelengths.

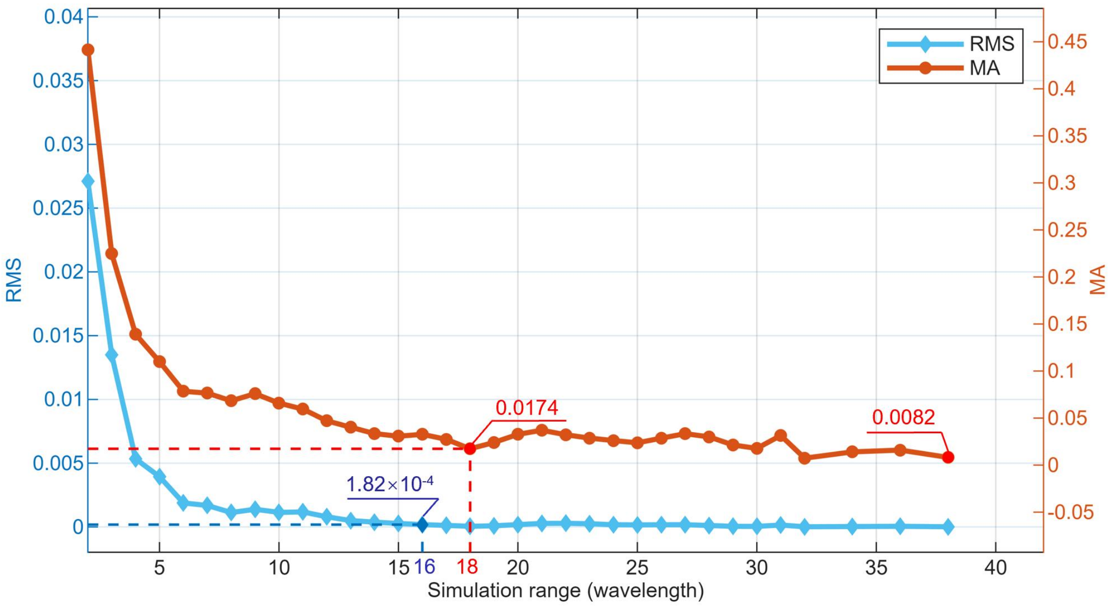

Fig. S4 Convergence of mask edge electromagnetic field deviation with FDTD simulation domain size.